World Academy of Science, Engineering and Technology
International Journal of Mechanical and Mechatronics Engineering
Vol:11, No:4, 2017

Human Intraocular Thermal Field in Action with Different Boundary Conditions Considering Aqueous Humor and Vitreous Humor Fluid Flow

Dara Singh, Keikhosrow Firouzbakhsh, Mohammad Taghi Ahmadian

***Abstract*—**In this study, a validated 3D finite volume model of human eye is developed to study the fluid flow and heat transfer in the human eye at steady state conditions. For this purpose, discretized bio-heat transfer equation coupled with Boussinesq equation is analyzed with different anatomical, environmental, and physiological conditions. It is demonstrated that the fluid circulation is formed as a result of thermal gradients in various regions of eye. It is also shown that posterior region of the human eye is less affected by the ambient conditions compared to the anterior segment which is sensitive to the ambient conditions and also to the way the gravitational field is defined compared to the geometry of the eye making the circulations and the thermal field complicated in transient states. The effect of variation in material and boundary conditions guides us to the conclusion that thermal field of a healthy and non-healthy eye can be distinguished via computer simulations.

***Keywords*—**Bio-heat, Boussinesq, conduction, convection, eye.

NOMENCLATURE

s	Specific heat ($\frac{J}{kgK}$)
E	Tear evaporation rate (W/m^2)
g	Acceleration due to gravity (m/s^2)
h	Heat transfer coefficient ($\frac{W}{m^2K}$)
$\dot{m}$	Mass flow rate (kg/s)
Q	Heat generation rate (W/m^3)
t	Time (s)
T	Temperature (K)
u, v, w	Velocity components (m/s)
x, y, z	Cartesian coordinates (m)
ρ	Density (kg/m^3)
μ	Dynamic viscosity ($\frac{kg}{ms}$)
σ	Stefan-Boltzmann constant ($\frac{W}{(m^2K^4)}$)

Subscripts

0	Reference
amb	ambient
b	body
bl	blood
c	cornea
s	Region on sclera

Greek Symbols

β	Coefficient of thermal expansion (1/K)
ε	Emissivity
ζ	Thermal conductivity across boundary ($\frac{W}{mK}$)
η	Unit outward normal (m)

Dara Singh is with Mechanical Engineering Department, at University of Kentucky, Lexington, KY, 40506-0503 USA (corresponding author, phone: 859-447-4950; e-mail: dara.singh@uky.edu).

Keikhosrow Firouzbakhsh and Mohammad Taghi Ahmadian are with Department of Mechanical Engineering, Sharif University of Technology, Tehran, Iran (e-mail: firoozbakhsh@sharif.edu, ahmadian@sharif.edu).

I. INTRODUCTION

TEMPERATURE field in any living organ is a good indicator of any biological malfunctioning. In the case of human eye, thermal disturbances are more prominent due to inadequate blood flow though the eye and lack of skin covering as a protecting layer. Insufficient blood flow and possible tumors in the interior part of the eye make this organ more susceptible compared to other organs. Even weak thermal or mechanical shocks can have huge effects.

With the advent of advanced computational technologies, simulation of the heat distribution in the human eye has become popular in last two decades. Pennes' bio-heat equations have been traditionally the governing laws used in the finite difference time domain method (FDTD). Taflove and Brodwin [1] used the FDTD to calculate the transient solutions of the temperature distribution in a microwave irradiated on human eye. They assumed a constant convection heat transfer coefficient over the entire surface of the eyeball (see Fig. 1). However, in their work, the frontal section and the posterior sections have not been properly distinguished and assuming the homogeneous uniform body, the effect of different thermal impedances of different layers has also been neglected. In addition, they considered that the initial temperature of the entire eye is uniform. This assumption is inappropriate since the transient solution is reliant on the initial steady state temperature field of the organ. Al-Badwaihy and Youssef [2] also examined the thermal effects of microwave radiation on human eye under steady state temperature distribution. They demonstrated an analytical method of solution for the steady state temperature distribution of rabbit eye. Their main achievement was that they assumed a combined (convection and radiation) heat transfer coefficients. Later, Lagendijk [3] introduced a mathematical model based on the FDTD method to compute the transient and steady state temperature distributions in the normal unexposed the human eye. In addition, he generalized the data that he obtained in the measurements on the rabbit eye to the human eye. Hirata et al. [4] investigated on the effect of electromagnetic waves in altering the temperature field of the

human eye employing the FDTD method. Their model still lacked discrete structure, and the results are not satisfactory with today's computational technology.

Emery et al. [5] and Guy et al. [6] were among the pioneers in employing FEM. Their investigations were on the rabbit eyes subjected to electromagnetic waves. Scott [7] and Amara [8] analyzed the steady state temperature profile by employing a two-dimensional (2D) FEM of the human eye. Scott [9] studied 2D FEM model of temperature variation in the intra-ocular media in the human eye when exposed to infrared. Their model considered both transient and steady state solutions. Their investigation emphasized on the importance of blinking effect and evaporation rates on the temperature of the human eye. In the both of his investigations, models with discrete regions were employed. Even in recent studies, the initial temperature (or steady state temperatures) has been considered to be constant. As an example, Chua et al. [10] presented a numerical model to predict temperature distribution within the human eye subjected to a laser source using only four ocular tissues. Hence, the geometry of the eye was not complete. Flyckt et al. [11] studied the impact of blood flow on temperature distribution in the human eye.

Recently, some investigations have been made on convection heat transfer coefficient due to the blood flow over human eye sclera. Ng et al. [12], [13], Ng and Ooi [14], and Ooi et al. [15] presented 3D and 2D models. A transient model for corneal laser surgery (thermokeratoplasty) using boundary element method was presented by Ooi et al. [16]. Narasimhan et al. [17] investigated on transient simulations of heat transfer in the human eye undergoing laser surgery. Their model lacked the effect of natural heat convection phenomena occurring in aqueous humour and vitreous humour.

Ooi and Ng [18] investigated the effects of natural convection in the human eye on temperature distribution considering the aqueous humor, where they modeled aqueous humor as a fluid. Heys and Barocas [19] and Kumar et al. [20] have also made investigations on flow of aqueous humour. They demonstrated that circulation of aqueous humor causes an asymmetric temperature distribution in models of the anterior chamber only. Karampatzakis and Samaras [21] investigated on a more realistic 3D model considering only aqueous humor as the flowing body. Meanwhile, Shafahi and Vafai [22] studied human eye response to thermal disturbances considering aqueous humor fluid flow in a 2D model of the human eye. However, in that study, the effect of vitreous humor fluid flows and the 3D flows in human eye temperature distribution is neglected.

In this study, a half eye 3D model with axisymmetric finite volume numerical model based on the Pennes' bio-heat equation is used. For a more realistic study, equations are coupled with Boussinesq equations. The present discretized human eye model is developed to explore the steady state temperature of a human eye when exposed to different thermal conditions rooting from various biological conditions of the body, material properties, including the lens conductivity, the effect of choroidal blood convection, the direction of the acceleration due to gravity and the alterations in the external thermal properties on thermal field distribution, and fluid flow in the human eye.

II. Methodology

This section is divided into the two subsections. In the first part, a brief note on geometry of the study case is given. In the second part, the governing differential equation on the geometry is introduced. Finally, details on boundary conditions and componential method are described.

A. Model Development

The left lobe of the human eye is represented in a 3D model created in Gambit 2.2.30 by rotating the 2D model presented in Fig. 2 through 180 degrees. In fact, this model closely resembles the dimensions used by Ooi et al. [16]. The pupillary axis has a length of 25.2 mm, and the vertical diameter is 24 mm. The model shown in Fig. 1 consists of six different sub-domains; namely, the cornea with an average thickness of 0.57 mm, aqueous humor, iris, lens, vitreous humor, and sclera. In human eye, there exist two additional tiny layers beneath the sclera, called the choroid and retina. In order to avoid excessive complications, these two tiny layers have been disregarded in this study. Each organelle (sub-domain) is considered to be homogeneous and isotropic.

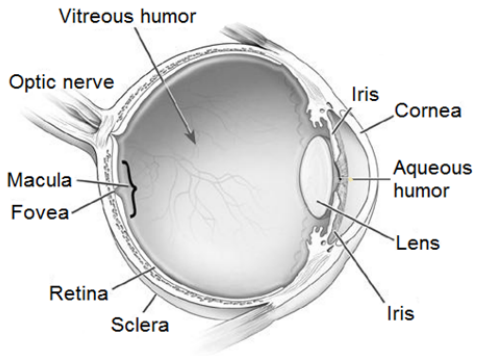

Fig. 1 Anatomy of a human eye [26]

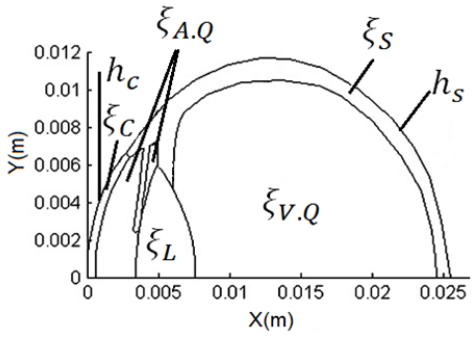

Fig. 2 Domains of the human eye model [16]

B. Mathematical Formulation

The thermal distribution in human eye under different environmental condition can be derived by solving the energy equation. The Pennes' bio-heat transfer equation [23] is

$$\rho C\frac{\partial T}{\partial t} = \nabla(\lambda \nabla T) + Q + \dot{m}_{bl}C_{bl}(T_{bl} - T) \quad (1)$$

Equation (1) is solved with the appropriate boundary conditions in [23]. The field variables are defined in Nomenclature. In (1), the second term stands for the heat generated by an internal or external source in the eye domain. Since there is no external heat source, it is assumed that there is no heat source or sink [17]. The last term in (1) is the blood perfusion arising due to blood flow through the tissue. This term contributes to the choroidal blood flow at the rear of the eye as a cooling mechanism during thermal trauma or during any physical injuries to the eye. The steady state temperature distribution is found by solving (1) without the temporal heat generation and blood perfusion terms [17].

Fluid convection is considered to be present in the aqueous humour as well as in the vitreous humour. In this study, a steady 3D incompressible Navier–Stokes equations are employed to simulate the laminar flow inside the respective sections of the of the human eye model. The equations are:

$$\rho\left(\frac{\partial u}{\partial t} + u\frac{\partial u}{\partial x} + v\frac{\partial u}{\partial y} + w\frac{\partial u}{\partial z}\right) = -\frac{\partial P}{\partial x} + \mu\left(\frac{\partial^2 u}{\partial x^2} + \frac{\partial^2 u}{\partial y^2} + \frac{\partial^2 u}{\partial z^2}\right) + \rho g_x \quad (2a)$$

$$\rho\left(\frac{\partial v}{\partial t} + u\frac{\partial v}{\partial x} + v\frac{\partial v}{\partial y} + w\frac{\partial v}{\partial z}\right) = -\frac{\partial P}{\partial y} + \mu\left(\frac{\partial^2 v}{\partial x^2} + \frac{\partial^2 v}{\partial y^2} + \frac{\partial^2 v}{\partial z^2}\right) + \rho g_y \quad (2b)$$

$$\rho\left(\frac{\partial v}{\partial t} + u\frac{\partial v}{\partial x} + v\frac{\partial v}{\partial y} + w\frac{\partial v}{\partial z}\right) = -\frac{\partial P}{\partial y} + \mu\left(\frac{\partial^2 v}{\partial x^2} + \frac{\partial^2 v}{\partial y^2} + \frac{\partial^2 v}{\partial z^2}\right) + \rho g_y \quad (2c)$$

TABLE I
MATERIAL PROPERTIES

Region	Thermal Conductivity ζ	Density ρ	Specific Heat c	Dynamic Viscosity μ	Thermal Expansion β
Cornea	0.58[5]	1050[7]	4178[25]	N.A	N.A
Aqueous humour	0.58[5]	996[7]	3997[7]	0.00074[18]	0.000337
Lens	0.40[3]	1050[25]	3000[3]	N.A	N.A
Vitreous humour	0.60[7]	1000[7]	4178[7]	0.00074[18]	0.000337
sclera	1.00[24]	1100[24]	3180[24]	N.A	N.A

Temperature gradient is the most prominent mechanism enhancing the fluid dynamics in a human eye. The buoyancy due to the change of density (due to the change of temperature rather than pressure) is modeled using the Boussinesq approximation as in [21], [22]. The following equation from the literature has been utilized in this research;

$$\rho = \rho_0[1 - \beta(T - T_0)] \quad (3)$$

The index "0" in (3) refers to the reference temperature, and details are provided in Table I. The reference temperature was assumed as 25℃. For the dynamic fluid flow of aqueous humor and vitreous humor, the value of dynamic viscosity of $\mu = 0.00074\ \mathrm{Ns/m^2}$ and that of the linear thermal expansion, $\beta = 0.000337\ 1/\mathrm{K}$. In fact, the aqueous humors as well as the vitreous humor are composed of 98-99% water so the assumed properties can be approximated with water. Ooi and Ng [18] used the given values for modeling the aqueous humour fluid flow. In addition, continuity equation,

$$\nabla . v = 0 \quad (4)$$

should also be satisfied. The assumed flow in our model is laminar. Therefore, by the constitutive law for laminar fluid dynamics [18], continuity of the flow should be satisfied in the regions where convection exists.

C. Boundary Conditions

Heat transfer between the cornea and the ambient environment is modeled by a single boundary condition. The region between the sclera and the rest of the human body was also modeled by a single boundary condition. Fig. 2 clearly illustrates the boundary conditions. In order to solve (1), it is assumed that

$$\zeta\frac{\partial T_c}{\partial \eta} = h_c(T_c - T_{amb}) \quad (5)$$

where h_c is defined by;

$$h_c = \left[E_{vap} + h_{amb}(T_c - T_{amb}) + \varepsilon\sigma(T_c^4 - T_{amb}^4)\right]/[T_c - T_{amb}] \quad (6)$$

The boundary conditions on the sclera is

$$\zeta\frac{\partial T_s}{\partial \eta} = h_s(T_s - T_b) \quad (7)$$

Also on the plane dividing the eye into two half lobes (left and right), it was assumed that there exists no heat transfer. Hence, there is no heat flux and it can be mathematically depicted by

$$\frac{\partial T_c}{\partial \eta} = 0 \quad (8)$$

It is assumed on the boundary of the sub-domains that

$$\zeta_i\frac{\partial T_i}{\partial \eta} = \zeta_j\frac{\partial T_j}{\partial \eta} \quad (9a)$$

$$T_i = T_{j,} \quad (9b)$$

where the sub-domain i and j convene through a common boundary between the cross section of the half eye and outer boundary.

D. Numerical Method

The model is developed in Gambit 2.2.30. The model comprised of 741,100 tetrahedral cells facilitating the Finite Volume Method (FVM) software of Fluent 6.3.26 to do the calculations with the highest precision possible on a 2.27 GHz Intel(R) Core(TM) i3 CPU and 4 GB ram. The calculations were performed on double precision mode in Fluent, since the dimensions of domain as well as primary variables including temperature were small. The convergence criterion is set as 10^{-6} for continuity and velocities. In addition, it is required to satisfy 10^{-9}considering energy criterion. Furthermore, a second order formulation is employed for the energy equation solver due to its significance in this problem.

III. Model Validation

The present half three-dimensional FVM model was validated with Scott's [7] 2D FEM model, considering the same material properties and the boundary conditions as considered by Scott's [7]. He employed a model with 25.4mm in length along with the pupillary axis; just 0.2mm longer than the present model. He considered a body temperature of 37°C and an ambient temperature of 20°C as the control parameters. Table II clarifies the regions and the material properties used by Scott [7] in his FE model.

TABLE II
PHYSICAL PARAMETERS OF THE OCULAR MEDIA USED BY SCOTT [7]

Media	K ($\frac{W}{m°C}$)	c ($\frac{J}{Kg°C}$)	ρ ($\frac{kg}{(m^3)}$)
Cornea	0.58	4178	1050
Aqueous humour	0.58	3997	1000
Lens	0.40	3000	1050
Vitreous humour	0.603	4178	1000

As shown in Table II, Scott did not consider the sclera or the iris. The other control parameters of the Scott's include; $h_s = 65 W/m^2°C$, $h_c = 10\ W/m^2°C$ $E_{vap} 40\ W/m^2$, $\sigma = 5.6697 \times 10^{-8}\ W/m^2K^4$ and $\varepsilon = 0.975$. The results in Fig. 3 are in good agreement with the Scott's model. The present model has also been validated by Lagendijk's [3] revised model presented by Flyckt et al. [11].

In fact, Flyckt et al. studied dependency of temperature distribution in the human eye considering the impact of the blood flow [11]. In the Lagendijk's revised model, a single heat transfer coefficient for sclera and the cornea was used.

TABLE III
VALIDATION WITH LAGENDIJK'S [3] REVISED MODEL PRESENTED BY FLYCKT [11]

Methodology			Cornea Temperature		Sclera Temperature	
h_c	h_s	Power Density	Revised Lagendijk	Present Model	Revised Lagendijk	Present Model
20	65	0	32.7	33.5	36.7	36.8
20	65	$60x10^3$	38.6	38.9	40.4	40.6
20	65	$120x10^3$	44.7	44.4	44.2	44.3
20	65	$180x10^3$	50.8	49.8	48.0	49.0
20	250	$60x10^3$	36.8	37.0	38.0	37.9
20	250	$120x10^3$	40.6	40.1	40.0	38.9
20	250	$180x10^3$	44.4	43.1	40.0	39.9
20	300	$60x10^3$	36.6	36.9	37.8	37.8
20	300	$120x10^3$	40.3	39.8	38.7	38.6
20	300	$180x10^3$	43.9	42.7	39.5	39.4

The single heat transfer coefficient incorporates the effects of thermal radiation, convection as well as evaporation through the corneal surface. It also considers the effect of blood flow on the surface of sclera. In addition, heuristic power densities were incorporated in order to study the cooling effects of the sclera. Moreover, the present model has also been validated with some of the experimental results obtained in the last century as presented in Table III. The experimental results are obtained employing different thermal measurement techniques for the measurement of the corneal temperature. It has been stressed to use the same boundary conditions like ambient temperature and blood temperature observed by them to compare the central corneal and average corneal temperature.

IV. Result and Discussions

In this section, temperature field and fluid flow pattern in the human eye under different biological and environmental conditions are studied. Since the fluid inside human eye is assumed to take part in convection, therefore it is important to understand the effect of gravity on natural convection in the eye. Different orientation of the eye with respect to gravity can lead to different flow field. In the following subsections, only two (i.e., horizontal and vertical) positions of the eye with respect to the gravitational direction are considered. Next, the effect of ambient temperature on the thermal field is studied. Since there are variations in heat conduction coefficient in different individuals and different ages, another subsection is also allotted for exploring the effect of heat conduction coefficient on thermal field of the human eye. Finally, effect of blood temperature and dynamics of blood flow is investigated.

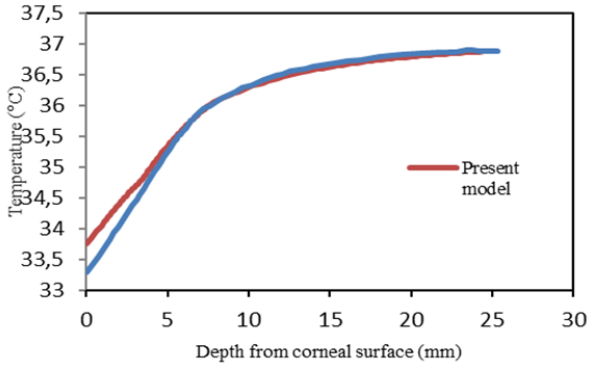

Fig. 3 Comparison of the present model with respect to that of Scott's presence of convection phenomena inside the human eye aqueous humor

A. Thermal Field in Standing Position

In the half eye 3D model presented, the control values were assumed to be as follows; $h_s = 65\ W/m^2°C, h_c = 20\ W/m^2°C$, $T_s = 37°C$ and $T_C = 25°C$. Fig. 4 shows the thermal distribution on the human eye when the person is upright; i.e., the gravity acts along the negative Y-axis. In this model, it is assumed that there is no blinking. Hence, the eye is considered to be in the steady state. It can be observed that due to buoyancy, the warmer fluid which is lighter arises to the upper levels. Therefore, the upper levels of the eye are relatively warmer. It is also noticed that prominently due to the convection and nonlinearity of the geometry, iso-levels of the human eye may experience different temperatures. The non-symmetric thermal distribution of cornea about its radial axis is distinguishable in Fig. 4. In the older models, since the natural convection of the eye had not been considered, the diagram of the thermal variation along the pupillary axis is different. In fact, due to the convection, the curves do not look

as smooth as earlier works (compare Figs. 3 and 6). As Fig. 6 illustrates, 3 mm to 4mm from the corneal surface, there is a sudden change in the temperature field along the central axis of the human eye. This is due to the presence of convection phenomena inside the human eye aqueous humor.

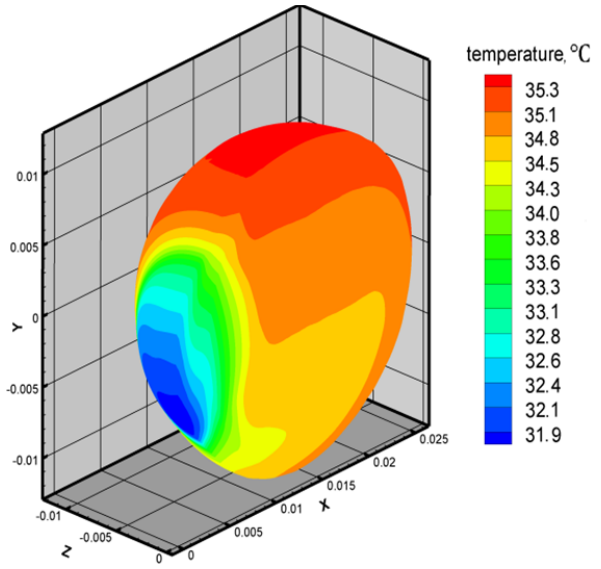

Fig. 4 Steady states thermal distribution of human eye when the gravity acts along the negative Y-axis

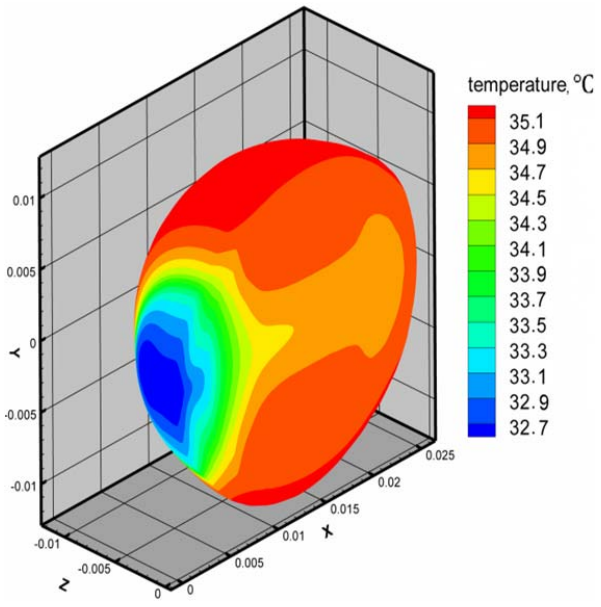

Fig. 5 Steady state thermal distribution of human eye when the gravity acts along the positive X-axis

B. Thermal Field in Sleeping Position

With the same control parameters as previous sub-section, but with the gravitational force vector acting on the positive X-axis, the thermal distribution of the human eye has been depicted in Fig. 5. This figure illustrates that the thermal distribution about the papillary axis is symmetric and is similar to the position experienced while the subject is in recumbent position. In fact, the lowest temperature is found to be at the center of the cornea. This condition is experienced when a person is lying with the eyes toward up. In this simulation, the involuntary movements of the eye which might influence the dynamics of the fluid flow have been neglected.

C. Thermal Field with Varying Ambient Condition

Heat exchange to the environment is done through three main mechanisms; namely, through radiation, evaporation of tears, and the convection of heat via the movement of air in the surrounding. In this modeling, it is assumed that all these heat transfers occur through a single heat transfer phenomena. Therefore, an equivalent convection heat transfer coefficient is introduced. Reasonable heat transfer coefficients have been employed to check the thermal variation of the human eye in interaction with the ambient boundary change. Fig. 6 depicts the sensitivity of thermal variation along the pupillary axis in action with the change of ambient temperature. Evidently, the changes in the ambient parameters do not alter the inner thermal field of the human eye as compared with the corneal surface. Fig. 7 illustrates the change in the equivalent heat transfer coefficient to the free environment. Fig. 6 shows that possession of the nonlinear geometry extremely alters the central corneal temperature variation when fluctuation in ambient heat transfer coefficient is imposed. It means that changing the ambient temperature from 30°C to 15°C may alter the corneal surface temperature only by 2°C. Therefore, changes in the ambient temperature only alter the frontal part of the human eye. The thermal field of the posterior region is, however, dominated by human circulatory fluid properties. Fig. 8 shows the central corneal temperature as a function of heat transfer coefficient. This figure shows close to linear relationship between heat transfer coefficient and the central corneal temperature.

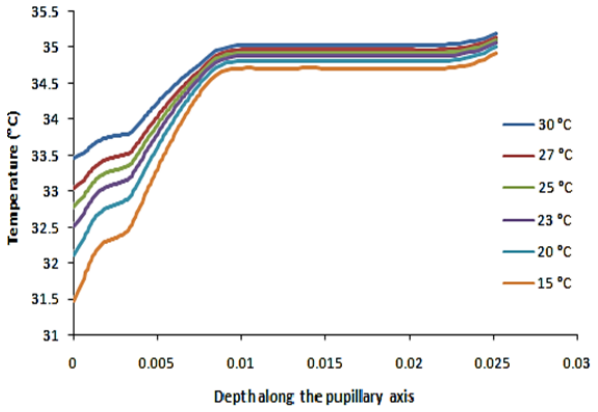

Fig. 6 Thermal variation along the pupillary axis of a human eye in contact to the different ambient temperatures

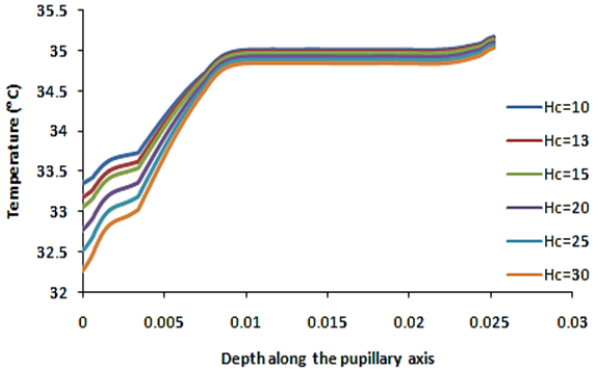

Fig. 7 Thermal variation along pupillary axis of a human eye in contact to the ambient with different heat transfer coefficient

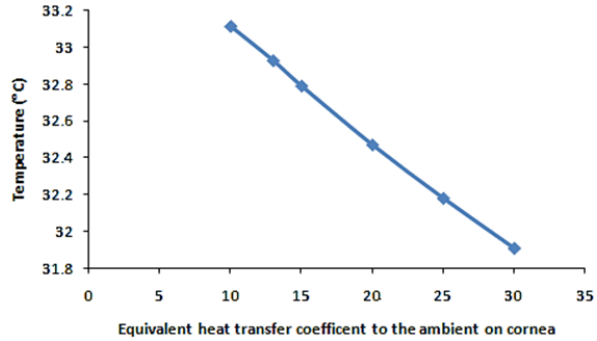

Fig. 8 Temperature variation at the center of human eye cornea with respect to the variation of ambient heat transfer coefficient

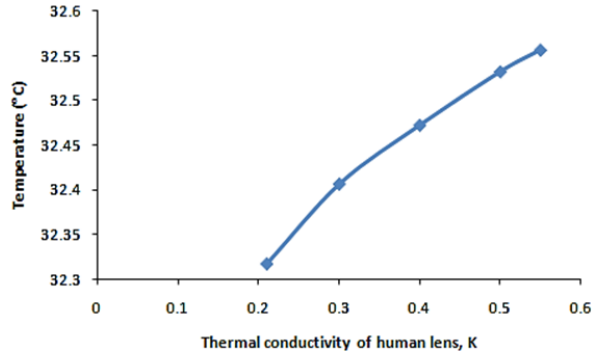

Fig. 9 Temperature variation at the center of human eye cornea with respect to the change in the conductivity of the lens

D. Thermal Field with Varying Lens Resistivity

Exploring the human eye lens, it is perceptible that the physical properties of the human eye lens keep changing with the age. As an example, myopia (nearsightedness) is an outcome of this phenomenon. In this study, the nonlinearity of these variations has been neglected for simplicity. The conductivity of the human eye lens has been considered linearly isotropic. However, the magnitude is varied to investigate its role on the thermal field variation of the human eye. Fig. 10 demonstrates that there is no perceptible change in the thermal variation of the posterior segment of the human eye. The resistance of human eye lens to the conduction leads to variation in the anterior segment's heat stability. It is interesting to notice that there are some nonlinearities considering the central corneal temperature in changing the changes in human eye lens heat transfer conductivity (see Fig. 9).

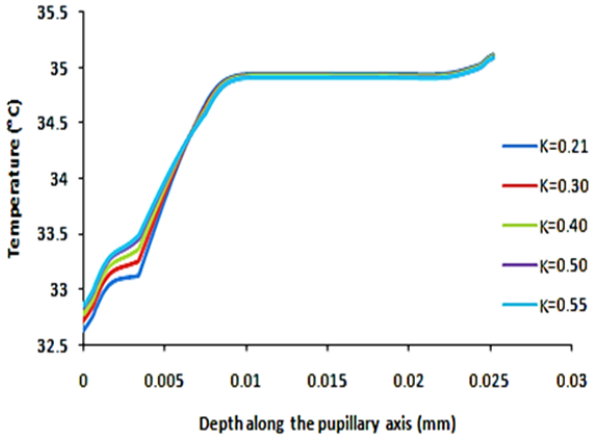

Fig. 10 Thermal variation along the pupillary axis of a human eye with different lens conductivity

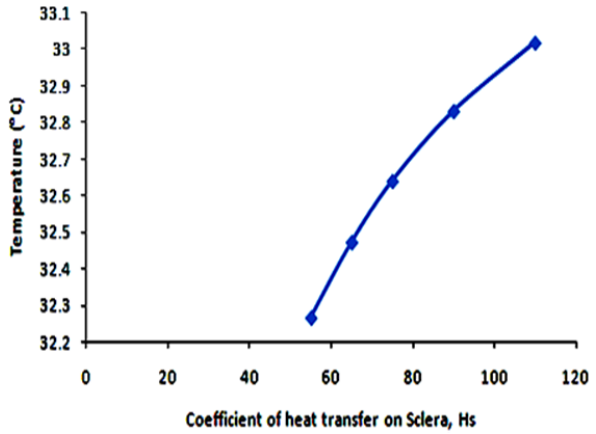

Fig. 11 Temperature variation at the center of human eye cornea with respect to the variation of blood heat transfer coefficient on sclera

E. Thermal Field with Varying Blood Properties

The thermal properties of the human eye depend upon the rates of blood perfusion and the temperature of the blood. However, the blood flow depends upon the heart beat rate and might be influenced by the trauma or infections. Meanwhile, the blood temperature also depends on the blood metabolism. In the present model, it is assumed that the eye is "heated up" by the flow of blood over the sclera. As discussed in [7], the blood perfusion can be modeled by an equivalent heat transfer coefficient centering$h_s = 65\ \mathrm{W/m^2{}^\circ C}$. In this research, the effect of heat transfer coefficient of the eye to body ranges from $55\ \mathrm{W/m^2{}^\circ C}$ to $110\ \mathrm{W/m^2{}^\circ C}$ as shown in Fig. 10. The blood temperature is also assumed to range from 35°C to 39°C. However, the control parameter is taken as 37°C. Fig. 10 reveals that the change in blood heat transfer coefficient may exhibit nonlinearity up to some extent. In contrast, Fig. 11 emphasizes that the central corneal temperature is predictable. Fig. 12 shows that the changes in the blood temperature do no cause tremendous changes in the thermal profile of the human

eye but, a shift in the overall thermal field is inevitable. Moreover, Fig. 13 shows the dependency of the temperature along papillary axis on blood temperature flowing over the sclera. This figure reveals that there is a slight change in thermal profile as blood temperature changes. In the other words, on the cornea, the temperature is dependent on both the source temperature and the ambient temperature, while deep inside the eye the thermal field is only a function of blood temperature.

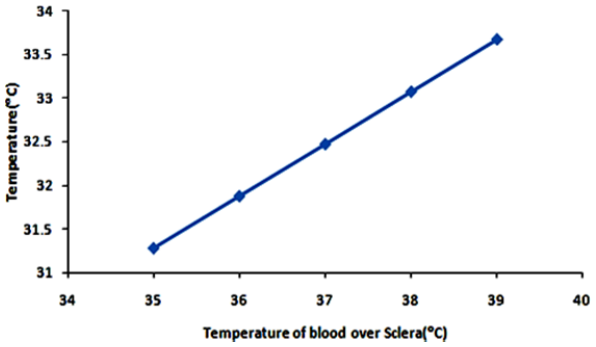

Fig. 12 Temperature variation at the center of human eye cornea with respect to the variation of blood temperature on sclera

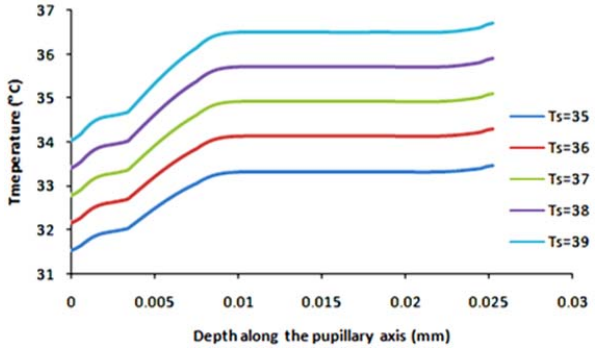

Fig. 13 Thermal variation along pupillary axis of a human eye with variation in blood temperature

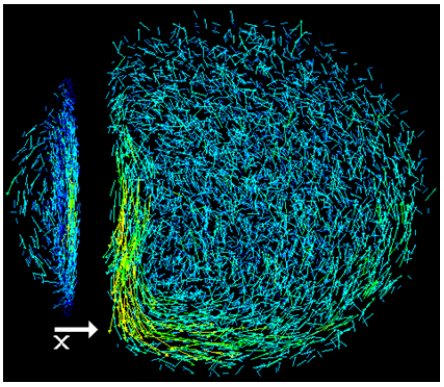

Fig. 14 Velocity vector in human eye when the gravity acting along the negative Y-axis

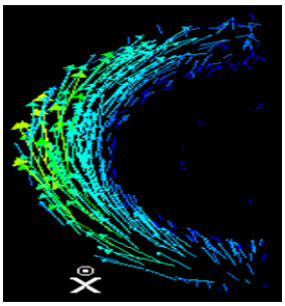

Fig. 15 Velocity vector in the vertical plane perpendicular to the pupillary axis beside the iris

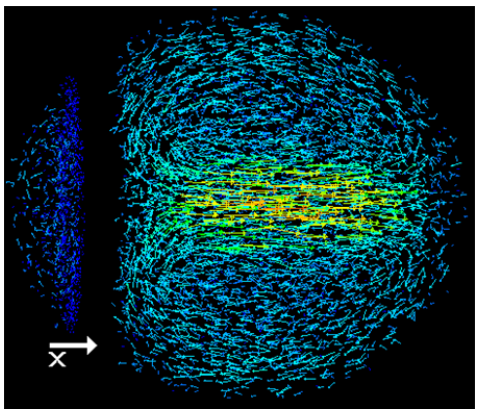

Fig. 16 Velocity vector in human eye when the gravity acting along the positive X-axis

F. Thermal Field with Varying Internal Convection

There are two fluid bodies in the human eye. The fluid in the anterior segment is called Aqueous humor and the fluid in the posterior segment is called vitreous humor. Since there are no blood vessels inside the human eye, these fluid act as a media for the transportation of vital materials. Water comprises the major portion of them and is contained by 98-99% in volume. Figs. 14-16 show the velocity vectors of the fluid particles in the human eye. Short descriptions are captioned below each figure. For instance, Fig. 14 demonstrates the overall flow over the human eye. The magnitude of the highest particle velocity reaches the order of millimeters per second. Figs. 14-16 convey that the fluid tends to "climb up" the warmer walls and "swoop down" along the colder walls. Hence, in the vitreous humor the fluid tends to climb up the sclera while it settles down when reaching the region around the lens. In the aqueous humor region, the same phenomena are more evident since the thermal variation between the boundaries play imperative role in dictating the flow conditions. It is evident from Fig. 15 that shifting the plane just a few millimeters towards the posterior segment of the anterior chamber, just beside the iris, causes aqueous humor to move in the upward direct; hence, warming is taking place in this case.

G. Thermal Field with Varying Gravity

Fig. 16 depicts the general fluid movement due to the thermal gradient in the human eye when the gravity acts along the X-axis in the originally defined coordinate system. In this

case, due the radial symmetric about the X-axis, the flow is symmetric about the pupillary axis of the eye. Here, also the mechanism is almost same as the previous model with a small modification. After getting cooled, the denser fluid settles down completing a circular motion. These circular motions are noticed in the Fig. 16. In the case of vitreous humor, the fluid after cooling tends to settle down along the central corneal axis, since it is furthest from the warmer "wall" of the sclera. Aqueous humor gets cooler when it contacts to the corneal walls. Hence it settles down along the vertical axis. In addition, when it is close to the lens and the iris, it also exhibits radially outward movement. It also "climbs up" the corneal wall where it gradually loses its heat to the wall, finally reaches the corneal center where it has potentially lost it thermal heat and starts to settle down (move toward positive X-axis) repeating the cycle. Meanwhile, Figs. 14-16 also elicit the fact that the aqueous fluid attains centrifugal motion.

V. Conclusion and Summary

In the present work, the human eye has been modeled in a 3D domain considering the fact that the human eye without the loss of generality is axially symmetric about its pupillary axis. Hence, in order to study the phenomena taking place in the human eye and also in order to conserve computational time, the domain is limited to left half of human eye by imposing symmetric boundary conditions at central plane of the eye. Moreover, the dynamics of the fluid have also been accounted in order to get a more precise view of the heat transfer inside the human eye. For simplicity, the energy source of the human eye has been limited to the thermal heat received from the blood vessels surrounding the sclera. Also, it is assumed that the heat is transferred to the surrounding through the corneal surface. Therefore, an equivalent heat transfer coefficient has been defined on the corneal surface to the ambient. The physical properties of the different parts of the human eye have been extracted from the present literature and articles. The main motivation of this study is its completeness, i.e., coupling heat transfer and the dynamics of the fluids bodies present inside the human eye.

As a result, it has been demonstrated that the thermal field of the human eye can be influenced by the many biological and physiological factors that can be described and interpreted as boundary temperature, material properties, and heat transfer coefficients, in addition to variation in gravitational force vector. It can also be inferred that other movements causing any form of acceleration might alter the dynamic flow of heat inside the human eye, thereby changing the thermal field of the eye. It can also be concluded that any obstacle or abnormal objects like tumors can alter the thermal field of the eye, shedding lights on potentially new method of diagnosis in medical worlds.

References

[1] A. Taflove, and M. Brodwin, "Computation of the electromagnetic fields and induced temperatures within a model of the microwave-irradiated human eye." *IEEE Transactions on Microwave Theory and Techniques,* 23, 1975: pp. 888–896.

[2] K. A. Al-Badwaihy, and A. B. A. Youssef, "Biological thermal effect of microwave radiation on human eye," in: C.C. Johnson, M.L. Shore (Eds.), *Biological Effects of Electromagnetic Waves*, 1, 1976: pp. 61–78.

[3] J. W. Lagendijk, "A mathematical model to calculate temperature distributions in human and rabbit eyes during hyperthermic treatment," *Physics in Medicine and Biology*, 27, 1982: pp. 1301–1311.

[4] A. Hirata, S. Matsuyama, and T. Shiozawa, "Temperature rises in the human eye exposed to EM waves in the frequency range 0.6–6 GHz," *IEEE Transactions on Electromagnetic Compatibility,* 42, 2000: pp. 386–393.

[5] A. F. Emery, P. Kramar, A. W. Guy, and J. C. Lin, "Microwave 466 induced temperature rises in rabbit eyes in cataract research." *Journal of Heat Transfer,* 97, 1975: pp. 123–128.

[6] A. Guy, J. C. Lin, and P. O. Kramar, "Emery AF., "Effect of 2450 MHz radiation on the rabbit eye," *IEEE Transactions on Microwave Theory and Techniques,* 23 1975: pp. 492–498.

[7] J. A. Scott, "A finite element model of heat transport in the human eye,' *Physics in Medicine and Biology*, 331988: pp. 227–241.

[8] E. H. Amara, "Numerical investigations on thermal effects of laser ocular media interaction." *International Journal of Heat and Mass Transfer,* 38, 1995: pp. 2479–88.

[9] J. A. Scott, "The computation of temperature rises in the human eye induced by infrared radiation," *Physics in Medicine and Biology*. 33, 1988: pp. 243–257.

[10] K. J. Chua, J. C. Ho, S. K. Chou, and M. R. Islam, "On the study of the temperature distribution within a human eye subjected to a laser source," *International Communications in Heat and Mass Transfer*, 32, 2005: pp. 1057–1065.

[11] V. M .M. Flyckt, B. W. Raaymakers, and J. J. W. Lagendijk, "Modelling the impact of blood flow on temperature distribution in the human eye and the orbit: fixed heat transfer coefficients versus the Pennesbioheat model versus discrete blood vessels," *Physics in Medicine and Biology*, 51, 2006: pp. 5007–5021.

[12] E. Y. K. Ng, and E. H. Ooi, "Ocular surface temperature: a 3D FEM prediction using bioheat equation," *Computers in Biology and Medicine*. 37, 2007: pp. 829–835.

[13] E. Y. K. Ng, E. H. Ooi, and U. Rajendrarcharya, "A comparative study between the two-dimensional and three-dimensional human eye models," *Mathematical and Computer Modelling*, 48, 2008: pp. 712–720.

[14] E. Y. K. Ng, and E. H. Ooi, "FEM simulation of the eye structure with bioheat analysis," *Computer Methods and Programs in Biomedicine,* 82, 2006: pp. 268–276.

[15] E. H. Ooi, W. T. Ang, and E. Y. K. Ng, "Bioheat transfer in the human eye: a boundary element approach," *Engineering Analysis with Boundary Elements,* 31, 2007: pp. 494–500.

[16] E. H. Ooi, W. T. Ang, and E. Y. K. Ng, "A boundary element model of the human eye undergoing laser thermokeratoplasty," *Computers in Biology and Medicine.* 38, 2008: pp. 727–737

[17] A. Narasimhan, K. K. Jha, and L. Gopal, "Transient simulations of heat transfer in human eye undergoing laser surgery". *International Journal of Heat and Mass Transfer* 53, 2010: pp. 482–490.

[18] E. H. Ooi and E. Y. Ng, "Simulation of aqueous humor hydrodynamics in human eye heattransfer". *Computers in Biology and Medicine*, 38, 2007: pp. 252-262.

[19] J. J. Heys, and V. H. Barocas, "A Boussinesq model of natural convection in the human eye and the formation of Krukenberg's spindle," *Annals of Biomedical Engineering*.30. 2001: pp. 392-40.

[20] S. Kumar, S. Acharya, R Beuerman, and A. Palkama, "Numerical solution of ocular fluid dynamics in a rabbit eye: parametric effects," *Annals of Biomedical Engineering*, 34, 2006: pp. 530-44.

[21] A. Karampatzakis, and T. Samaras, "Numerical model of heat transfer in the human eye with consideration of fluid dynamics of the aqueous humour," *Physics in Medicine and Biology*, 55, 2010: pp. 5653–5665.

[22] M. Shafahi, and K. Vafai, "Human Eye Response to Thermal Disturbances," *Journal of Heat Transfer*, 133, 2011.

[23] H. H. Pennes, "Analysis of tissue and arterial blood temperatures in the resting human forearm," *Journal of Applied Physiology*. 85, 1998: pp. 5–34.

[24] U. Cicekli, 'Computational model for heat transfer in the human eye using the finite element method," *M.Sc. Thesis, Department of Civil & Environmental Engineering, Louisiana State University*, 2003.

[25] P. S. Neelakantaswamy, and K. P. Ramakrishnan, "Microwave-induced hazardous nonlinear thermo-elastic vibrations of the ocular lens in the human eye", *Journal of Biomechanics* 12, 1979: pp. 205–210.

[26] American foundation of Blind @http://www.familyconnect.org/info/after-the-diagnosis/working-with-medical-professionals/the-human-eye/135, last update June/11/2014.